Acta Biomaterialia 19 (2015) 100–111

Contents lists available at ScienceDirect

Acta Biomaterialia

journal homepage: www.elsevier.com/locate/actabiomat

Development of next generation of therapeutic IFN-α2b via genetic code expansion

Bo Zhang, Huan Xu, Jingxian Chen, Yongxiang Zheng, Yiming Wu, Longlong Si, Ling Wu, Chuanling Zhang, Gang Xia, Lihe Zhang, Demin Zhou *

State Key Laboratory of Natural and Biomimetic Drugs, School of Pharmaceutical Sciences, Peking University, Beijing 100191, China

ARTICLE INFO

Article history:
Received 6 November 2014
Received in revised form 8 February 2015
Accepted 3 March 2015
Available online 11 March 2015

Keywords:
Site-specific PEGylation
Interferon-α2b
Genetic code expansion
Bio-orthogonal conjugation

ABSTRACT

With the aim to overcome the heterogeneity associated with marketed IFN-α2b PEGylates and optimize the size of the PEG moiety and the site of PEGylation, we develop a viable and facile platform through genetic code expansion for PEGylation of IFN-α2b at any chosen site(s). This approach includes site-specific incorporation of an azide-bearing amino acid into IFN-α2b followed by orthogonal and stoichiometric conjugation of a variety of PEGs via a copper-free click reaction. By this approach, only the chosen site(s) within IFN-α2b is consistently PEGylated under mild conditions, leading to a single and homogenous conjugate. Furthermore, it makes the structure–activity relationship study of IFN-α2b possible by which the opposite effects of PEGylation on the biological and pharmacological properties are optimized. Upon re-examination of the PEGylated IFN-α2b isomers carrying different sizes of PEG at different sites, we find mono-PEGylates at H34, A74 and E107 with a 20-, 10- and 10-kDa PEG moiety, respectively, have both higher biological activities and better PK profiles than others. These might represent the direction for development of the next generation of PEGylated IFN-α2b.

1. Introduction

Interferons (IFNs) are a group of closely related cellular proteins generated and released by host cells in response to the presence of pathogens such as viruses, bacteria, parasites or tumor cells [1]. About ten distinct IFNs have been identified in mammals and seven of them are found from humans [2]. Several subtypes of IFNs are now developing as drugs for the treatment of a variety of infectious diseases and cancers [3]. In fact, IFN-α2b, a type I-IFN that binds to the cell surface IFN-α2b receptor, is the best-studied one and the recombinant IFN-α2b has been in market for the treatment of hepatitis C infection over one decade. Standard IFN-α2b therapy has a short half-life that requires subcutaneous injection daily or 3 times weekly to maintain effective levels in the blood [3,4]. The short half-life of IFN-α2b has led to the development of longer lasting preparations by the attachment of a large polyethylene glycol (PEG) molecule directly to IFN-α. Two different commercial preparations of PEG-IFN-α, PEG-INTRON® and Pegasys®, have been developed for clinical use. Both have achieved long half-lives upon PEGylation with 12- and 40-kDa PEG moieties, respectively, that permit once weekly administration [5,6].

PEGylation is usually achieved by tethering PEG to the reactive amino acids of target proteins such as lysine, cysteine, histidine, arginine, aspartic acid etc [7,8]. However, most of these amino acids are relatively abundant, for example, 10 lysine and 4 cysteine residues in IFN-α2b. Consequently, PEGylation of IFN-α2b via these amino acids usually results in a complex mixture of conjugates with different number and distribution of bound PEG chains [5,6,9]. It has been reported that ~47% of the PEG molecules in PEG-INTRON® are attached to H34 and the remaining are attached to K31, K83, K121, K131, K134 and the N-terminal cysteine residue [5,10,11]. It has also been reported that the major component of PEG-INTRON® is not stable due to the PEG-H34 bond, which undergoes hydrolysis in aqueous solution, resulting in the dissociation of PEG from the protein [12]. For the Pegasys®, a complex mixture of four major PEG-protein isoforms are identified with the PEG moiety at K31, K121, K131, and K134 and several minor isoforms at other sites [6,13]. Even PEGylation at a particular amino acid residue, mono-, di- and numerous higher-PEGylated conjugates were obtained [14]. It should be noted that the various positional isomers and mono-, di- and multiply-PEGylated IFN-α2b species have different specific activities, even as low as 1–7% of wild-type IFN-α2b, and PK profiles [14,15]. For such a heterogeneous product,

* Corresponding author at: School of Pharmaceutical Sciences, Peking University, No. 38, Xueyuan Road, Beijing 100191, China. Tel./fax: +86 10 8280 5857.
E-mail address: deminzhou@bjmu.edu.cn (D. Zhou).

http://dx.doi.org/10.1016/j.actbio.2015.03.002
1742-7061/

quality control and batch-to-batch reproducibility is often difficult to achieve. From the perspective of the product consistency and quality control required in modern drug production and regulatory approval, site-specific PEGylation leading to a single, well-defined conjugate offers clear advantages [16].

In an effort to overcome the heterogeneity associated with PEGylation of IFN-α2b, various conjugation techniques have been introduced in recent years including PEGylation at N- or C-terminal of IFN-α2b [10–16]. In particularly, site-specific introduction of a free cysteine followed by PEGylation of the added cysteine residue via a maleimide chemistry has been reported [17,18]. Despite the significance of this approach for PEGylation at any defined site, however, a limitation for this approach is apparent, particularly, the potential formation of a disulfide bond between the added cysteine and the constitutive cysteine residues in the target protein. In addition, the PEGylated reaction should be carefully designed and performed so that only the added cysteine but not the constitutive cysteine residues is PEGylated. Recently, it is reported that cysteine-mediated maleimide conjugated linker is intrinsically unstable [19,20], which may not maximize the potential benefits from PEGylation.

As a multi-billion dollar annual business with growing interest from both emerging biotechnology and established multinational pharmaceutical companies, there is great scientific and commercial interest in introducing various innovations to improve the biomedical efficacy and quality of IFNs [10]. In this study, we develop a facile platform through genetic code expansion [21,22] for PEGylation of IFN-α2b at any chosen site(s). Our approach involved two key steps (Fig. 1): incorporation of an azido-bearing amino acid [22,23] through genetic code expansion at various sites on the surface of the protein as a chemical handle; orthogonal conjugation of a variety of PEGs with IFN-α2b, site-specifically and stoichiometrically, via a strain-promoted alkyne-azide cycloaddition [24,25]. By this approach, homogenous PEGylation at only the chosen site(s) with the formation of a much stable linker between IFN-α2b and PEG moiety is consistently obtained, avoiding non-selective and less stable conjugations [19,26]. Furthermore, this approach provides a viable platform for systematic structure–activity exploration of IFN-α2b PEGylates, via different sizes of PEG at different sites, to optimize the effects of PEGylation on the biological and pharmacological properties. Upon re-examination of positional isomers of the PEGylated IFN-α2b, we found mono-PEGylates at H34, A74 and E107 with a 20-, 10- and 10-kDa PEG moiety, respectively, have both higher biological activities and better PK profiles. These might represent the direction for the development of the next generation of therapeutic IFN-α2b.

2. Materials and methods

2.1. General materials

Top 10 strains were used to clone and propagate plasmid DNA. Miniprep and maxiprep kits (*Qiagen*) were used to harvest and purify plasmid DNA. Go-TagGreenMaster Mix (*Promega*) and PCR clean-up System (*Promega*) were used to perform PCR and DNA fragment purification. QuickChange Lightning Site-Directed mutagenesis kit (*Agilent*) was used to generate site-directed mutations. Nε-2-azideoethyloxycarbonyl-L-lysine (NAEK) was synthesized as previously reported [23]. The linear 5, 10 and 20 kDa mPEG-NH_2 and the branched 40 kDa $(mPEG)_2$-NH_2, approximately 20 kDa per branch, were purchased from Kai Zheng Inc. (*Beijing, China*). The 4-dibenzocyclooctynol (DIBO) and DIBO-PEGs were synthesized as previously reported [25]. The commercial PEG-INTRON (12-kDa PEG-IFN-α2b) was manufactured by Schering-Plough Corp. (*Kenilworth, NJ*). The IFN-α2b standard was purchased from PBL InterferonSource Inc. (U.S.).

2.2. Molecular biology and production of IFN-α2b

The optimized gene encoding IFN-α2b [27] was synthesized by SanBoYuanZhi Inc. (Beijing, China) and cloned into vector pET21-a(+) within sites of NdeI and XhoI to generate pET21-IFN-WT. A 6× His tag was added at the C-terminal for affinity purification [28]. BL21(DE3), BL21(AI) and OrigamiB(DE3) were used as host strains for IFN-α2b expression. Generally, the strain hosting pET-IFN-α2b-WT was inoculated into 2 ml Luria–Bertani (LB) medium containing 100 μg/ml ampicillin and grown at 220 rpm and 37 °C. Then the overnight *E. coli* cultures were diluted to an optical density in 2× YT medium and incubated at 37 °C. When optical densities of the cultures reached ~0.5(OD_{600}), IPTG was added to a final concentration of 0.5 mM. After overnight induction at 24 °C, cells were harvested by centrifugation and re-suspended in His-Bind buffer (20 mM phosphate, pH 8.0, 500 mM NaCl, 20 mM imidazole). Protein extraction was performed by passing cells through a Microfluidizer 2 times at 1200 bar with cooling. The supernatant was collected by centrifugation and the pellets were re-suspended in PBS buffer. The samples were analyzed on 15% SDS–PAGE gel followed by CoomassieBlue staining under reducing conditions.

To generate plasmids encoding NAEK-containing hIFN variants at different positions, stop codon TAG was introduced by site-directed PCR mutagenesis to each corresponding position. The obtained mutant plasmid, pET-IFN-α2b-TAG, was transformed into

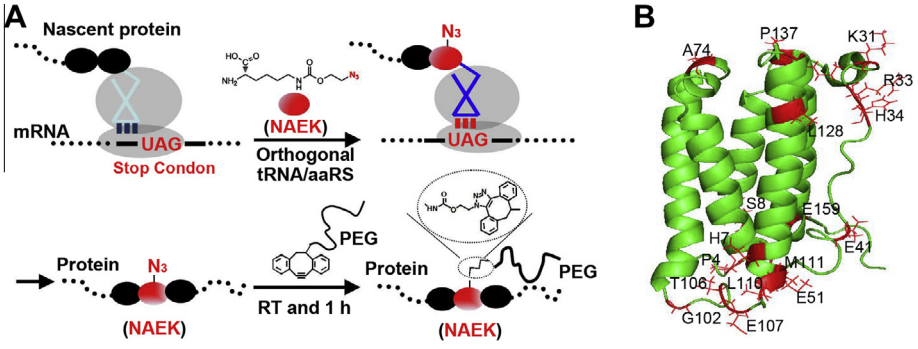

Fig. 1. Schematic diagrams of genetic code expansion-mediated site-specific PEGylation of IFN-α2b. (A) Briefly, an orthogonal amber suppressor tRNA, aminoacyl-tRNA synthetase (aaRS) pair is used to site-specifically incorporate unnatural amino acid (NAEK) in response to an amber nonsense codon. The azido group of NAEK can be coupled to PEG via a strain-promoted alkyne-azide cycloaddition, forming a stable triazole linkage, which occurs readily under physiological conditions in the absence of auxiliary reagents. (B) Schematic representation of the PEGylation sites in IFN-α2b (Crystal structure of IFN-α2b was down loaded from the PDB data base, PDB number: 2KZ1).

OrigamiB(DE3) cells alone with pSURAR-YAV plasmid, which contained the expanded genetic code system for an amber codon-suppressing tRNAPyl and NAEK-specific aminoacyl tRNA synthetase. Expression of NAEK-bearing IFN-α2b variants was similar as the expression of wild-type hIFN except the addition of NAEK in the medium; when OD_{600} reached to 0.5, NAEK was added to a final concentration of 1 mM and then protein expression was induced by IPTG and L-Arabinose at a final concentration of 0.5 mM and 0.1%, respectively, 0.5 h later.

2.3. Protein purification and PEGylation

The general procedure for purification of His-tag IFN-α2b was as follows: the bacterial lysate, which was re-suspended in His-Bind buffer, passed through a microfluidizer 2 times. After centrifugation, the IFN-α2b protein in the supernatant was mixed with Ni–NTA His-Bind Resin (*Novagen*) for 2 h. Then the unbound proteins were washed away with 10 volumes of washing buffer (20 mM phosphate, pH 8.0, 500 mM NaCl, 60 mM imidazole). The IFN-α2b protein enriched by resin was eluted with the same buffer but containing 500 mM imidazole. The eluted pool was diluted at a proper concentration with the pH adjusted to 4.5 by glacial acetic acid, and then loaded onto an SOURCE 15S (GE Healthcare) column equilibrated in 20 mM sodium acetate, pH 4.5. IFN-α2b protein was eluted with a 10–30% linear gradient in 5CV. Eluent buffer contained the following: 20 mM sodium acetate, 2 M NaCl, pH 4.5. Main elution peak was pooled, concentrated, and buffer exchange into IFN preservation solution using HiTrap™ Desalting column (GE Healthcare). The general procedure for PEGylation of IFN was as follows: DIBO-PEG was added to the Cation-Exchange elution buffer in 20× molar excess to IFN protein and then shaken gently at 4 °C for 1–2 h. The PEGylation reaction was confirmed by SDS–PAGE analysis stained by CoomassieBlue dye and Iodide. The PEGylated IFN-α2b was then purified by Cation-Exchange chromatography at the same condition but longer gradient range (over 15CV) to remove unreacted PEG and IFN. The purity of PEGylated IFN-α2b protein obtained in this way was usually greater than 95%.

2.4. Far-UV circular dichroism (CD) analysis

The CD spectrum (Model J-810, JASCO, Japan) was used to determine whether the secondary structures of IFN was affected upon PEGylation. The wavelength range was from 190 to 250 nm and all samples were diluted to 0.3 μg/μl with phosphate buffer. Each spectrum was scanned 3 times and the average spectrum was plotted. The experimental data were analyzed by CDpro software according to the CDSSTR analysis program.

2.5. Stability analysis

The thermal stability was determined as previously described [29]. Briefly, the wild-type, mutant and various IFN-α2b PEGylates were separately diluted to 0.3 μg/μl in PBS and then heated at 65 °C in a heat block. The heat-induced aggregation was monitored by measuring the apparent absorbance at 405 nm at time intervals of 5, 10, 15, 20 and 25 min. Test of the trypsin degradation resistance was carried out as previously reported [30]. Briefly, 16 μl of wild-type and PEGylated IFN-α2b at 0.2 μg/μl in sodium bicarbonate buffer were each mixed with 4 μl of trypsin dissolved at 0.16 μg/μl of the same buffer at room temperature. At time intervals of 1, 2, 3 and 4 h, 5 μl of 5× Loading Buffer was added and heated at 99 °C for 10 min to stop the tryptic reaction. Densitometric analysis of CoomassieBlue staining was used to determine the ability of the PEGylation to protect IFN-α2b against trypsin degradation.

2.6. Surface plasmon resonance (SPR) analysis

Receptor binding affinities were measured by BIAcore 3000 (*GE*) using the CM5 sensor. Analyses of interactions between IFNs and IFNAR2 (*Invitrogen*) were performed in HBS buffer (10 mM HEPES, 3 mM EDTA, 150 mM NaCl, pH 7.4) at a flow rate of 30 μl/min. The extracellular (EC) portion of IFNAR2 was directly immobilized onto the surface of the sensor at pH 5.0. All samples were measured at six different concentrations ranging from 0.8 nM to 200 nM by serial 3-fold dilutions. Between the measurements, no regeneration was needed because the dissociation was completed within 10 min. The experimental data were fitted and analyzed using the BIA evaluation software by a simple one-to-one kinetic model.

2.7. Peptide mapping analysis

The site-specific UAA incorporation and PEG conjugation were confirmed by peptide mapping [10]. Following trypsin digestion of the purified WT-IFN-α2b (as control), E41NAEK-IFN-α2b (IFN bearing UAA at site 41), H34NAEK-IFN-α2b and 10-kDa H34NAEK-PEG-IFN-α2b overnight at 37 °C, the reaction was quenched by adding TFA. The tryptic peptides were re-suspended and separated by C18 RP-HPLC (Easy-nLC II, *Thermo Fisher Scientific*, *CA*) with in-line UV detection. Fractions were collected, dried down, and re-suspended in trifluoroacetic acid subsequently. Each fraction was separated with an analytical C18 column further. The peptide(s) were identified by MALDI (MS and MS–MS) analysis.

2.8. Antiproliferation assay

The human Daudi B cell line was purchased from ATCC (CCL-213) and maintained in RPMI 1640 media supplemented with 10% fetal bovine serum (FBS), 50 μg/ml streptomycin and 50 unit/ml penicillin. For measurement, serial 3-fold dilutions of samples ranging from 0.3 to 2100 pg/ml were prepared in medium and were added in triplicate into a 96-well microplate with 100 μl/well. The washed cells were diluted to 2×10^5 cells/ml and 100 μl was added to each well (2×10^4 cells). After incubation for 4 days at 37 °C, viable cell densities were detected by an ATP-dependent assay using CellTiter-Glo Luminescent Cell Viability Assay (*Promega*). The EC_{50} values were calculated by sigmoidal nonlinear regression fit using GraphPad Prism 5 software, independent of weight contribution from PEG.

2.9. Antiviral assay

The human lung adenocarcinoma cell line A549 (ATCC No. CCL-185) was cultured in DMEM media supplemented with 10% FBS, 50 μg/mL streptomycin and 50 units/mL penicillin (assay media). For the antiviral assay A549 cells were re-suspended at 3×10^5 - cells in assay media and then aliquoted at 100 μl/well (3×10^4) into 96-well microtiter plates. Twelve hours later, 100 μl of each protein sample was prepared in assay media and added to the test wells in serial 3-fold dilutions. Each protein sample was tested in duplicate. Control wells contained either cells (negative control) or cells and virus (positive control). The plates were incubated overnight at 37 °C. The media was then removed and the cells were infected with 100 μl encephalomyocarditis virus (EMCV). When cell death reached ~90% in the control wells after 36–48 h, viable cell densities were determined by the CellTiter-Glo Luminescent Cell Viability Assay. The relative potency of IFN-α2b and all the PEG-IFNs tested was determined by comparing the dose of the test preparation, which afforded 50% protection to infected cells, with the dose of control IFN-α2b reference standard (PBL), independent of weight contribution from PEG.

2.10. Pharmacokinetic study in rats

Pharmacokinetic properties of samples were determined following intravenous and subcutaneous administration in Sprague Dawley rats. Groups of two male rats, weighing approximately 300 g each, received a single intravenous injection (lateral tail vein) of a sample at a dose of 100 μg of protein/kg of body weight. At selected time points, blood samples (0.1 mL) were drawn into EDTA anticoagulant tubes. The blood samples were centrifuged, and the plasma samples were stored at −80 °C until analysis. A pre-dose sample (0 h) was drawn 1 day prior to injection of the test compounds. Plasma levels of the test proteins were quantitated using A549 antiviral assay as described above and the concentration of wild-type IFN-α2b in plasma after six half-lives was treated as background and normalized to 0. The pharmacokinetic study by subcutaneous dosing was performed in the same manner except that the protein samples were injected subcutaneously into the lateral sides of the rats. Pharmacokinetic parameters were analyzed using the kinetica 4.4 software. All animal experiments were performed in accordance with the guidelines by the Institutional Animal Care and Use Committee of the Peking University.

2.11. Statistical analysis

The student *t*-test has been used to determine the statistical difference between means of groups and *P* values <0.05 were considered significant. All quantitative data shown are average values with standard deviations from triplicate experiments ($n = 3$).

3. Results

3.1. Identification of a proper host cell for high expression of soluble IFN-α2b

The *E. coli* system has been the choice for expression of IFN-α2b due to the significantly higher yield [31]. However, IFN-α2b expressed in *E. coli* often precipitates as insoluble aggregates that are mis-folded and biologically inactive [32]. In order to identify a proper host cell that produces soluble IFN-α2b, we screened a series of strains that have been used for the expression of other soluble proteins. The expression profiles of IFN-α2b in BL21(DE3), BL21(AI) and Origami™ B (DE3), upon transfection with pET21a(+)-IFN-α2b, are shown in Fig. 2. It was found that Origami™ B (DE3) expressed ~3-fold more protein than BL21(DE3) and BL21(AI) (Fig. 2A). Furthermore, we found that around 60% of IFN-α2b expressed in Origami™ B (DE3) was soluble based on CoomassieBlue staining analysis (Fig. 2A). In contrast, less IFN-α2b was expressed in BL21(DE3) and BL21(AI) and most was present as a non-soluble form (>95%), consistent with the previous report [31]. Large-scale production of soluble IFN-α2b with a yield of ~50 mg/L in shake flasks was achieved by optimizing culture conditions as follows: Origami™ B (DE3) as the host strain, 2× YT as the medium, a final concentration of 0.5 mM IPTG as the inducer, and at 24 °C for overnight growth.

3.2. Site-specific incorporation of azido-bearing amino acid into IFN-α2b via genetic code expansion

Following identification of Origami™ B (DE3) as the host strain for expression of soluble IFN-α2b, we explored whether N-2-azideoethyloxycarbonyl-L-lysine (NAEK), an azido-bearing unnatural amino acid, could be genetically incorporated into a chosen site of IFN-α2b. The IFN-α2b-expressing vector, pET21a(+)-IFN-α2b, was mutated at the residue E41, a site randomly chosen as a representative, to the amber codon (TAG). The mutant vector, pET21a(+)-IFN-α2b-TAG(41), was transfected with pSURAR-YAV, a plasmid encoding amber codon-suppressing tRNA and NAEK-specific aminoacyl tRNA synthetase [23] into Origami™ B (DE3), which was then cultured in the presence of NAEK. A strong band was detected by CoomassieBlue staining and confirmed as IFN-α2b by Western blotting and molecular weight measurement (Fig. 2B). No expression of IFN-α2b was detected without NAEK in the culture medium, which supported the compatibility of genetic code expansion in engineering NAEK to the IFN-α2b protein. Incorporation of NAEK at site E41 was confirmed by peptide sequencing (Fig. 2C), i.e. a mass shift of approximately 112-Da (±1 Da), which was equal to the mass difference between glutamic residue and NAEK, was detected at this specific position. The optimized conditions for expression of the NAEK-carrying IFN-α2b were almost identical to that of wild-type IFN-α2b but with a supplement of NAEK (S Fig. 1). When the cell density reached 0.5 of OD_{600}, NAEK was added at a final concentration of 1 mM, followed by 0.5 mM IPTG and 0.1% L-Arabinose. By this approach, a consistent production of mutant IFN-α2b in a yield of 30 mg/L was obtained in shake flasks.

The facile replacement of E41 with NAEK suggested that genetic code expansion might be utilized for systematic engineering of IFN-α2b with NAEK at any defined site(s). Twenty residues were chosen as representatives for replacement by NAEK individually. Choice of these sites was dictated by their exposure locations (Fig. 1B). Similar as the mutation at site E41, the genetic code of each chosen amino acid was mutated to TAG. Then the mutant vectors were tested in parallel for their ability to incorporate NAEK at each of the chosen sites. CoomassieBlue staining indicated that the full length of IFN-α2b protein was detected for most of the mutant vectors. Quantification of NAEK incorporation yield indicated that the highest were associated with A74 and E113, over 95% relative to the IFN-α2b control, and the lowest were sites R125 and C29, less than 10% compared with the control (Fig. 2D). Other sites demonstrated intermediate yield, around 70–85% for sites H7, R33, H34, E41, E51, 107 and P137. The remaining sites, including P4, S8, K31, E78, G102, T106, L110, M111, L128, K133 and E159, exhibited yield from 30% to 50% relative to that of the IFN-α2b control.

We then investigated whether these IFN-α2b mutants still maintained their biological activity and determined at which sites incorporation of NAEK brought the minimal deleterious effect on activity. Cell Titer-Glo viability assay indicated that NAEK mutants at P4, H34, E41, E51, A74, E107, L110, M111, E113 and P137 exhibited comparable IC50 as that of wild-type IFN-α2b (Fig. 2E, averaging 14–26 pg/ml vs. 15.2 ± 5.6 pg/ml of WT-IFN). This result suggests those surface sites are functionally tolerant to NAEK modification. For sites H7, E78, T106, L128 and K133, the mutant IFN-α2b proteins exhibited 30–80% activity as compared with the wild-type IFN-α2b (averaging 28–40 pg/ml of IC50). This result suggests that these sites are also tolerant to NAEK modification with little significant reduction observed. For the remaining 5 sites, NAEK replacement led to loss of activity to less than 20% of the wild-type activity for S8, E159, K31 and G102 (Fig. 2E, IC50 > 45 pg/ml), indicating these residues are essential for maintaining protein conformation or they are involved in receptor-binding. In particular, residue R33 is directly involved in IFN-α2b and IFNR2 binding [33], and the least activity (~5%, IC50 = 266.4 ± 20.7 pg/ml) was observed after modification.

3.3. Development of an orthogonal and facile platform for site-specific PEGylation of IFN-α2b

We next investigated PEGylation of IFN-α2b via the incorporated NAEK. Incubation of 10-kDa DIBO-PEG with H34NAEK-IFN-α2b led to a predominant product (~95%) based on CoomassieBlue staining with an apparent molecular weight of

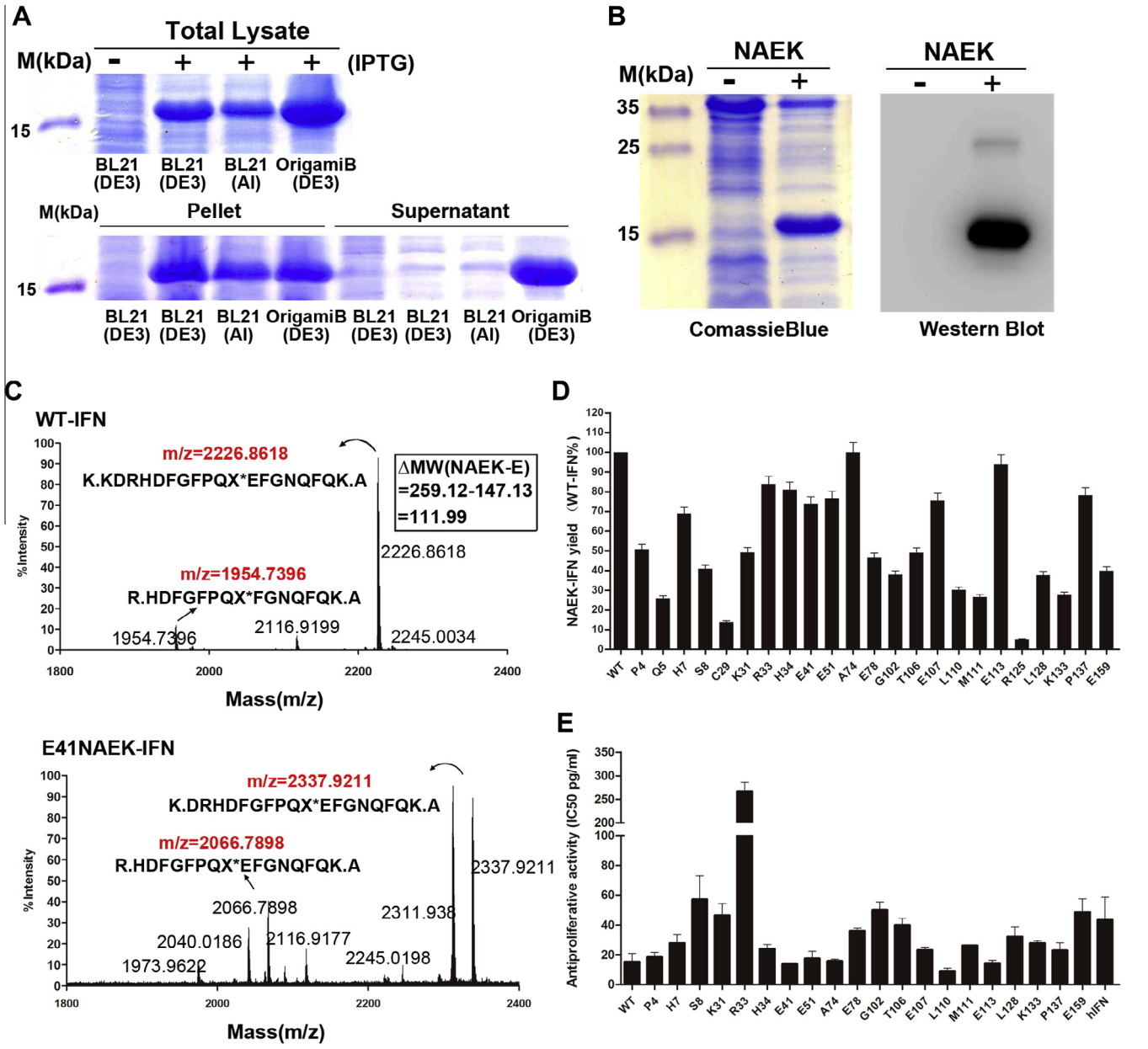

Fig. 2. Site-specific incorporation of NAEK in IFN-α2b. (A) SDS–PAGE analysis of IFN-α2b expression for the identification of a proper *E. coli* strain to express soluble IFN-α2b. Strains include BL21(DE3), BL21(AI) and OrigamiB(DE3) as labeled in the gel. The non-induced BL21(DE3) was used as a negative control. (B) Analysis of NAEK-engineered IFN-α2b expression in OrigamiB(DE3) detected by CoomassieBlue staining and Western blotting, respectively. (C) Peptide sequencing of IFN-α2b for validation of the incorporation of NAEK at the chosen site. The purified proteins were analyzed by SDS–PAGE and the corresponding bands were excised for MS analysis. *X** denotes NAEK in E41NAEK-IFN or Glutamic in WT-IFN at the position of 41. *m*/*z* of peptides after tryptic digestion of E41NAEK-IFN: 2066 and 2337; *m*/*z* of peptides after trypsin digestion of WT-IFN: 1954 and 2226. (D) Comparisons of the incorporation efficiency of NAEK at different sites relative to WT-IFN. (E) Comparisons of the anti-proliferative activity of NAEK-engineered IFN-α2bs. WT means wild-type IFN-α2b prepared by us; hIFN means wild-type IFN-α2b purchased from PeproTech as positive control. All quantitative data shown are average values with standard deviations from triplicate experiments ($n = 3$).

~35 kDa (Fig. 3A). In a control experiment wherein wild-type IFN-α2b was incubated with DIBO-PEG, no such product was detected. Characterization of this product by iodide staining confirmed it as a PEGylated derivative of IFN-α2b (Fig. 3A) and thus demonstrated the critical role of NAEK in the PEGylation reaction. The selective attachment of a single 10 kDa PEG to IFN-α2b via NAEK was verified by MALDI-TOF mass spectrometry (MS): all peptides except the one containing NAEK were identified for PEG-IFN-α2b conjugate (S Fig. 2A). The observed much greater apparent molecular weight of 10-kDa PEG-IFN-α2b was potentially due to the hydrophilic and linear nature of the PEG moiety [22]. Further characterization of the NAEK-mediated PEGylation indicated that it was temperature- (4 °C to 37 °C) and pH- (2–12) independent and usually accomplished within 1 h (S Fig. 2B).

Optimization of the molar ratio of DIBO-PEG vs. IFN-α2b for PEGylation indicated that an increased degree of PEGylation was observed with increase of the molar excess of DIBO-PEG until at 1:20 (S Fig. 2B). This result suggested 20-fold of extra DIBO-PEG could be used for PEGylation of IFN-α2b. Accordingly, a 10-kDa PEG moiety was separately coupled to the active mutant proteins including P4NAEK-, H7NAEK-, E41NAEK-, E51NAEK-, A74NAEK-, E107NAEK-, E113NAEK- and P137NAEK-IFN-α2b (S Fig. 3). In addition, linear 5-, 10- and 20-kDa PEG moieties and a branched 40-kDa PEG moiety were also separately coupled to

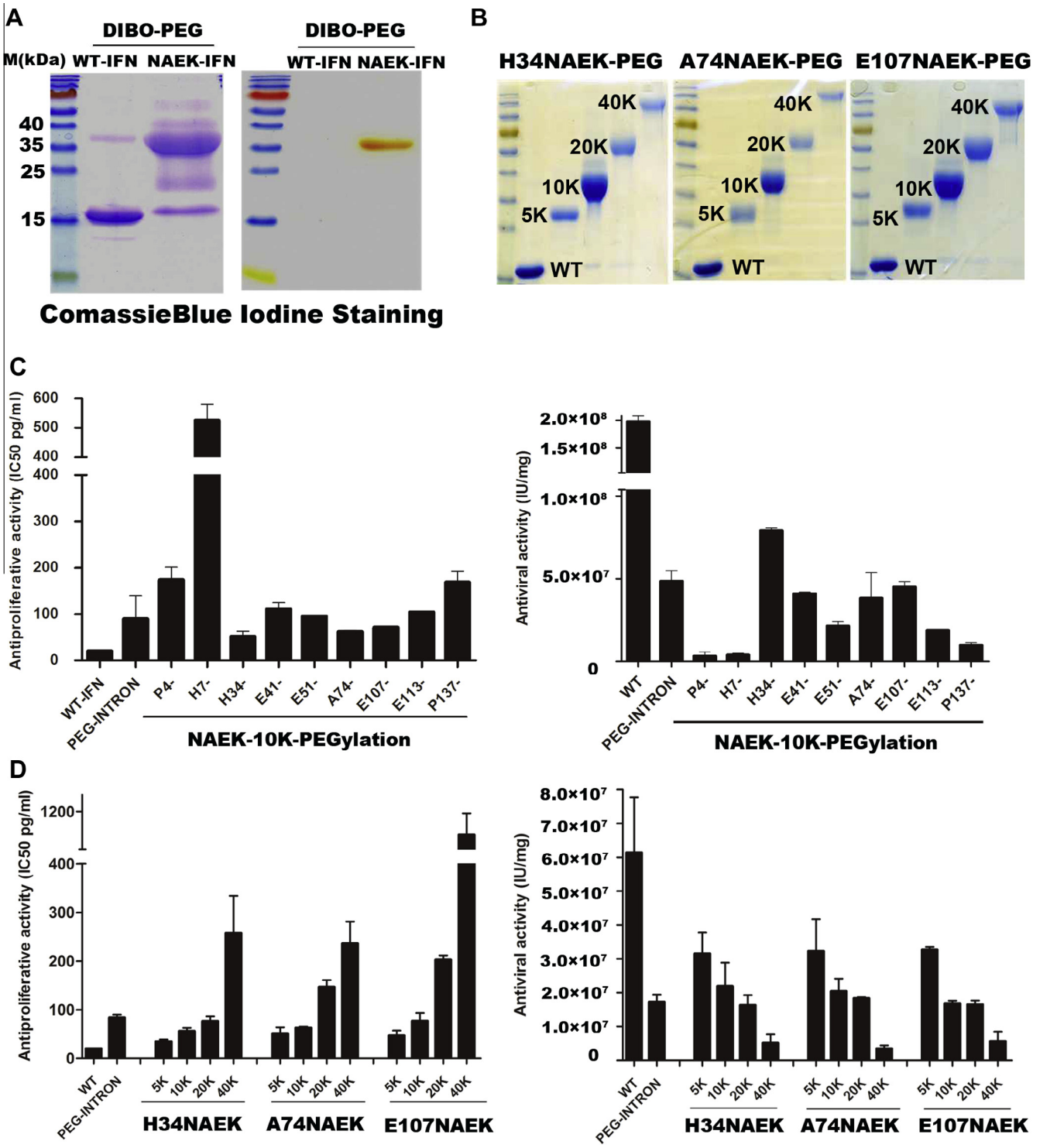

Fig. 3. NAEK-mediated PEGylation of IFN-α2b. (A) SDS–PAGE analysis of the conjugation product of H34NAEK- IFN-α2b and 10-kDa DIBO-PEG by CoomassieBlue and iodine staining, respectively. (B) Analysis of PEGylation products of IFN-α2b at site H34NAEK, A74NAEK and E107NAEK by different sizes of PEG moieties. The size of conjugated PEG moieties, 5, 10, 20 and 40 kDa, were labeled in gels. (C) Characterizations of the effect of PEGylated sites by a 10-kDa PEG moiety on the anti-proliferative and antiviral activities. (D) Characterization of the effect of PEG sizes on the anti-proliferative and antiviral activities of IFN-α2b. All quantitative data shown are average values with standard deviations from triplicate experiments ($n = 3$).

the most active H34NAEK-, A74NAEK- and E107NAEK-IFN-α2b (Fig. 3B). Comparing with the previous methods that always formed a complex mixture of 6–14 positional isomers [14], only one mono-PEGylated isomer was produced from each PEGylation reaction with the PEG moiety attached at the desired site (Fig. 3B).

3.4. The structure–activity relationship study of IFN-α2b PEGylates carrying different sizes of PEG at different sites

We first characterized the effect of PEGylation on structure of IFN-α2b. The circular dichroism (CD) spectra, which reflect conformation change of the protein, indicated that all 10-kDa

PEGylated IFN-α2b positional isomers showed a similar CD curve, especially in the near and far UV regions, as that of the wild-type IFN-α2b (S Fig. 4A and S Table 1). This result suggests that PEGylation at those sites causes no perturbation on structure and folding of IFN-α2b. We also measured the affinity of the 10-kDa PEGylated isomers to IFNAR2, one major receptor of IFN-α2b [34]. According to the K_D value, a consistent reduction in affinity was observed upon PEGylation and the P137NAEK PEGylated isomer exhibited the most reduction (40 nM vs. 4 nM), almost 10-fold decrease comparing with IFN-α2b (S Fig. 4B). The K_D value for the wild-type IFN-α2b was generally consistent with the previous literature value. For other PEGylated isomers, their affinity to IFNAR2 decreased by 3 to 6-fold, depending upon the PEGylation site (averaging 9–20 nM of K_D values). Whereas the NAEK-mediated PEGylation brings substantial reduction in IFN-α2b/IFNAR2 affinity, most of such PEGylated positional isomers were equivalent and even superior to the commercial PEG-INTRON in K_D value (29 nM). In addition, thermal aggregation assay showed that turbidity of IFN-α2b, even exposure to 65 °C up to 25 min, was significantly reduced by PEGylation, independent on the size of PEG. This result indicates that such PEGylation indeed enhances the thermal stability of IFN-α2b (S Fig. 4C).

We then investigated whether such PEGylated isomers of IFN-α2b still have the desired biological activities and at which site PEGylation brings the minimal deleterious effect on biological activities of IFN-α2b. According to the CellTiter-Glo assay, significant anti-proliferative activity was found for positional isomers of H34NAEK, A74NAEK and E107NAEK; all showed roughly 40% activity comparing with IFN-α2b but twofold higher than that of PEG-INTRON (Fig. 3C), while for positional isomers at E41NAEK, E51NAEK and E113NAEK, equivalent activity to PEG-INTRON was observed. Thus, these PEGylated isomers appear to have the potential to be developed as new versions of IFN-α2b therapeutics. For sites P4NAEK, H7NAEK and P137NAEK, PEGylation significantly attenuated the bioactivity (IC50 = 173.6 ± 27.7, 525.2 ± 55.1 and 168.6 ± 23.7; $P < 0.006$). The loss in biological activity for these 3 positional isomers seems not likely due to structural perturbation of the IFN-α2b (S Fig. 4A) but the poor binding to the receptor (S Fig. 4B).

Results obtained in the antiviral assay were similar to those in the anti-proliferation assay. PEGylation with a 10-kDa PEG molecule generally resulted in lower antiviral activity for all positional isomers (Fig. 3C). Even so, the H34NAEK PEGylated isomer still retained the highest activity ($7.9 \pm 0.15 \times 10^7$ IU/mg), 40% relative to that of IFN-α2b ($2.0 \pm 0.099 \times 10^8$ IU/mg) as compared with 25% for PEG-INTRON ($4.9 \pm 0.64 \times 10^7$ IU/mg), a value comparable with those previously reported [11,14]. Other positional isomers PEGylated at E107, E41 and A74 were also active and equivalent in antiviral activity to that of PEG-INTRON. For PEGylated isomers at P4NAEK and H7NAEK, much lower antiviral activity was detected ($3.5 \pm 2.3 \times 10^6$ and $4.1 \pm 1.0 \times 10^6$ IU/mg). Clearly, PEGylation sites strongly influence the antiviral activity. However, the higher anti-proliferative and antiviral activities associated with H34NAEK, A74NAEK and E107NAEK positional isomers suggested that these sites are favorable for PEGylation.

In order to investigate the effect of PEG size on IFN-α2b activity, three series of positional isomers PEGylated at H34NAEK, A74NAEK and E107NAEK were prepared by conjugating with different sizes of PEG. Anti-proliferation and antiviral assays showed the activities of 5-kDa PEG-IFN-α2b at H34NAEK were 57.8% and 51.3%, respectively, comparing with that of IFN-α2b, significantly higher than the corresponding 40-kDa PEG-IFN-α2b which exhibited just 7.8% and 8.3% activities ($P < 0.01$, Fig. 3D). The significant difference in activities in this study is consistent with previous observation – a progressive relationship exists between decreased activity and increased PEG size [11]. However, small reductions in activities were observed for PEG moieties ranging from 10- through 20-kDa (55.9 ± 6.8 vs. 76.1 ± 10.6 pg/ml in anti-proliferation assay), and the obtained PEGylated proteins exhibited 35.9–26.3% relative activities compared with IFN-α2b (anti-proliferation activities) (Fig. 3D). This result suggests that there is an upper limit of PEG size, probably 20-kDa, for the H34NAEK site; sizes lower than this had less effect on the biological activities of IFN-α2b. Similar trends of decreased biological activities associated with increased PEG sizes were also observed in A74NAEK and E107NAEK PEGylated isomers, especially for the 40-kDa PEGylated protein which showed 5.6% and 9.2% (antiviral) and 8.5% and 2.2% (anti-proliferation) relative activities of IFN-α2b (Fig. 3D). Exception was the different upper limit of the PEG size, 10-kDa for A74NAEK and E107NAEK (62.3 ± 2.9 or 77.6 ± 16.7 pg/ml of 10 kDa PEGylates and 146.6 ± 14.6 or 202.4 ± 9.1 pg/ml of 20 kDa PEGylates) positional isomer vs. 20-kDa for H34NAEK positional isomer, in the anti-proliferation assay. However, the diminished activity by 20-kDa PEG in the anti-proliferation assay was not observed in the antiviral assay. This 20-kDa PEGylated isomer was comparable to 10-kDa isomer, roughly 26% of the IFN-α2b activity in antiviral activity (Fig. 3D). Our data suggest that 20-kDa and 10-kDa are favorable sizes for PEGylation of IFN-α2b at H34NAEK and E107NAEK, respectively.

3.5. The pharmacological properties of PEGylated IFN-α2b

We first determined the effect of PEGylation sites on the pharmacokinetics (PK) of IFN-α2b. The 10-kDa PEGylated isomers at H34NAEK, A74NAEK and E107NAEK were utilized and their elimination curves upon a single intravenous (i.v.) injection are shown in Fig. 4A; their PK data are summarized in Table 1. As expected, the PEGylated isomers were superior to IFN-α2b with the clearance half-life extended from 1.5 to ~6.5 h, AUC was improved from 0.56 to ~30 μg/ml h and the elimination rate decreased from 2.4 to ~1.2 h^{-1} for all positional isomers tested. This is consistent with the previous report [17]. However, the roughly equivalent PK values within the variation of the assay for three PEGylated isomers at three different sites suggested that the significant PK gain is independent of the PEGylation sites.

We then determined the effect of PEG size on PK properties via exploring the PEGylated H34NAEK isomers from 5 through 40 kDa. The elimination curves upon a single intravenous injection indicated that the clearance half-life varied depending upon the sizes of the attached PEG moieties (Fig. 4B, Table 2). Both 40- and 20-kDa isomers exhibited a longer half-life, 14.4 and 21.5 h compared with 1.6 h for IFN-α2b, while the half-lives of 10- and 5-kDa isomers were 9.9 and 3.5 h, respectively. Clearly, the increased PEG size was highly effective to extend the half-life of IFN-α2b. However, the small increase for 40- vs. 20-kDa isomer (15.46 ± 6.0 vs. 21.55 ± 0.43) suggested an upper limit of PEG size for enhancing the residence time, probably ~20-kDa for site H34NAEK. Results obtained in the subcutaneous injection assay (s.v.) showed the similar trend as those for i.v. injection. The half-lives of 5-, 10-, 20- and 40-kDa PEGylated proteins in subcutaneous assay were 4-, 14-, 34- and 48-fold longer than that of IFN-α2b as compared with 2-, 6-, 9- and 14-fold obtained in i.v. injection assay (Fig. 4C). Thus, changes in PK values for PEGylated IFN-α2b appeared to be influenced by administration routes. The mean residence time (MRT), similar to the elimination half-life, was also increased upon conjugation of a long PEG moiety, more than a 3-, 8-, 15- and 30-fold (s.v.) increase when a 5-, 10, 20- or 40-kDa-PEG was respectively conjugated (Table 3). In general, a similar correlation in PK characteristics exists: the larger the PEG size, the more extended the PK parameters. Whereas PEGylation is highly effective for extending the half-life and MRT, it also attenuated absorption rates in the subcutaneous administration

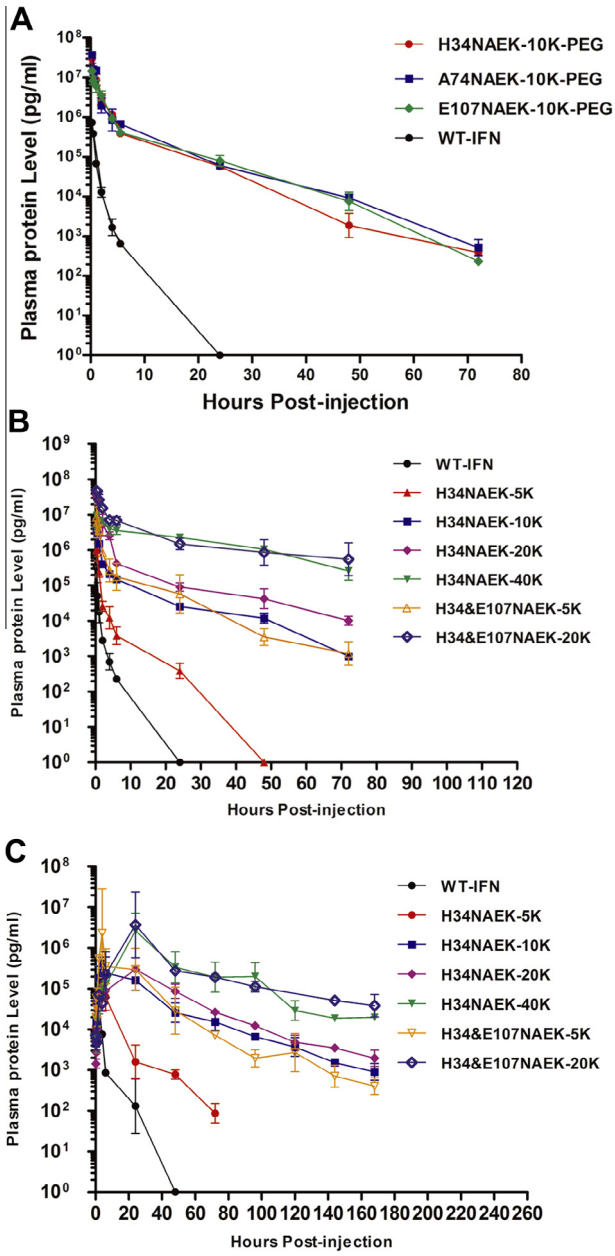

Fig. 4. Pharmacokinetic analysis of the effect of PEGylated sites and the size of PEG moieties on IFN-α2b. (A) Pharmacokinetic profiles of WT-IFN-α2b vs. 10-kDa PEGylated IFN-α2b at different sites via intravenous administration. Changes in plasma levels of (B) intravenous administration and (C) subcutaneous administration of WT- IFN-α2b, 5-, 10-, 20-, or 40-kDa mono-PEGylated IFN-α2b at H34NAEK and 5- or 20-kDa dual-PEGylated at H34NAEK and E107NAEK sites in Sprague–Dawley rats. All quantitative data shown are average values with standard deviations from triplicate experiments ($n = 3$).

Table 1
Summary of pharmacokinetic parameters of PEGylated IFN-α2b via intravenous administration.

Variant	$AUC_{0.25-\infty}$ (μg/ml) h	MRT (h)	$T_{1/2}$ (h)	Elimination rate (h^{-1})	Cl (ml/h)
WT	0.5 ± 0.1	0.5 ± 0.1	1.5 ± 0.8	2.4 ± 0.42	59.5 ± 7.0
H34-10K	34.4 ± 10.9	2.9 ± 0.8	6.5 ± 0.1	1.2 ± 0.1	0.9 ± 0.3
A74-10K	40.1 ± 7.4	2.7 ± 0.6	6.7 ± 0.4	1.3 ± 0.6	0.8 ± 0.1
E107-10K	25.5 ± 5.9	3.9 ± 0.4	6.3 ± 0.4	0.6 ± 0.01	1.2 ± 0.3

[35]. The peak time for 5-, 10-, 20- and 40-kDa PEGylated proteins were 3.5, 10, 20 and 30 h as compared with ~1 h for IFN-α2b (Table 3). This result indicated that the peak time is related to the size of PEG attached. The progressive relationship between enhanced PK parameters and increased PEG size suggest that the size of PEG moiety strongly influenced PK properties of PEGylated IFN-α2b.

3.6. The effect of dual- vs. mono-PEGylation on IFN-α2b activity

Following characterization of the effect of mono-PEGylation on IFN-α2b, we then determined whether the properties of IFN-α2b could be further improved upon double PEGylation. Similar to the process for incorporation of a single NAEK, the genetic codes of H34 and E107 within IFN-α2b were simultaneously changed to TAG. Transformation of such a IFN-α2b vector carrying two TAG codes into Origami(DE3) led to the production of a full-length IFN-α2b in a yield of ~10% of that for IFN-α2b. Incubation of 5 kDa DIBO-PEG with the purified IFN-α2b led to a conjugate with a molecular weight comparable to that of a 10-kDa mono-PEGylated isomer (S Fig. 5A). This result indicated that two NAEK residues and then two 5-kDa PEG moieties were engineered into a single IFN-α2b protein. By the same approach, two 10- and 20-kDa PEGs were also conjugated with a single IFN-α2b at sites 34 and 107, respectively (S Fig. 5A).

Circular dichroism and BIAcore affinity assay were utilized to test whether the conformation of IFN-α2b changed after dual PEGylation. We found very similar CD spectra for dual-PEGylated protein vs. mono-PEGylated protein (S Fig. 5B and S Table 1). In addition, data obtained from the BIAcore affinity assay indicated that the K_D values for di-5-kDa (6.3 nM) and di-20 kDa (27.4 nM) PEG-IFN-α2b were comparable to those of mono-5 kDa (3.8 and 10.2 nM for H34 and E107 respectively) and mono-20-kDa IFN-α2b (19.7 nM for H34 and 38.8 for E107), respectively (Fig. 5A). All these data supported that there was no structural change upon introduction of a second PEG moiety into IFN-α2b, at least in the tested sites. The trypsin digestion assay indicated the superiority of dual-PEGylated isomers: nearly 30% of di-5 kDa PEG-IFN-α2b was detected upon exposure to trypsin for 4 h, significantly higher than the just 5–10% for the mono-PEGylated isomers with either 5- or 10-kDa PEG ($P < 0.008$, Fig. 5B). Furthermore, data obtained from the PK studies indicated dual-PEGylated IFN-α2b was 2-fold higher in clearance half-life than mono-PEGylated isomers carrying the same size of PEG, and was equivalent to the mono-PEGylated isomer with the same molecular weight (Tables 2 and 3). Therefore, from the aspects of PK properties we conclude that dual-PEGylated isomers are generally superior to mono-PEGylated isomers.

However, inconsistent improvement was found for dual-PEGylated vs. mono-PEGylated IFN-α2b in biological activities, which were highly dependent on the PEG size. No superiority was found for di-5 kDa PEG-IFN-α2b vs. 5- or 10-kDa mono-PEGylated IFN-α2b due to their almost comparable activities in anti-proliferative and antiviral assays (Fig. 5C and D). However, di-20 kDa PEG-IFN-α2b became much less active – almost 4-fold lower than 20-kDa mono-PEGylated IFN-α2b (20.1 ± 3.6 vs. 3.5 ± 0.2 for H34 and 5.9 ± 0.7 for E107 respectively in anti-proliferative assay) and almost equivalent to the 40-kDa mono-PEGylated IFN-α2b (35.9 ± 10.0 and 22.3 ± 0.4 for H34 and E107 respectively) which has ~5% activity of IFN-α2b (Fig. 5C and D). It seems likely that conjugation of a second 20-kDa PEG with IFN-α2b brought significant deleterious effect on biological activities ($P < 0.008$, compared with WT-IFN). We concluded that PEGylation of IFN-α2b with two or more PEG of large size is not favorable due to the poor biological activities.

Table 2
Summary of pharmacokinetic parameters of mono-PEGylatedIFN-α2b at site H34 and dual-PEGylatedIFN-α2b at H34 and E107 with various PEGs via intravenous administration.

Variants	$AUC_{0.25-\infty}$ (μg/ml) h	MRT (h)	$T_{1/2}$ (h)	Elimination rate (h^{-1})	Cl (ml/h)
WT	0.5 ± 0.5	0.2 ± 0.2	1.6 ± 1.0	8.4 ± 7.8	103.1 ± 58.2
H34-5K	1.4 ± 0.8	0.8 ± 0.1	3.5 ± 0.1	3.9 ± 2.8	24.9 ± 12.7
H34-10K	6.5 ± 0.1	8.7 ± 1.2	9.9 ± 0.8	0.9 ± 0.01	4.6 ± 0.1
H34-20K	46.4 ± 13.0	11.6 ± 10.5	15.5 ± 6.0	1.0 ± 0.4	0.7 ± 0.2
H34-40K	147.0 ± 134.8	23.3 ± 11.6	21.6 ± 0.4	0.1 ± 0.07	0.4 ± 0.3
H34&E107-5K	15.5 ± 5.9	3.6 ± 2.0	9.9 ± 2.4	1.1 ± 0.9	2.1 ± 0.8
H34&E107-20K	164.4 ± 39.8	26.4 ± 13.9	16.6 ± 3.6	0.3 ± 0.05	0.1 ± 0.07

Table 3
Summary of pharmacokinetic parameters of mono-PEGylated IFN-α2b at site H34 and dual-PEGylated IFN-α2b at H34 and E107 with various PEGs via subcutaneous administration.

Variants	$AUC_{0.25-\infty}$ (μg/ml) h	T_{max} (h)	C_{max} (ng/ml)	MRT (h)	Elimination rate (h^{-1})	$T_{1/2}$ (h)	Cl (ml/h)
WT	0.2 ± 0.02	1.1 ± 0.05	53.2 ± 9.6	1.3 ± 0.2	0.8 ± 0.1	0.6 ± 0.01	195.3 ± 32.7
H34-5K	1.3 ± 0.9	3.6 ± 0.02	128.6 ± 90.6	4.3 ± 0.3	0.3 ± 0.01	2.1 ± 0.2	30.5 ± 20.6
H34-10K	6.5 ± 0.8	10.0 ± 1.9	248.0 ± 77.2	10.5 ± 3.0	0.1 ± 0.03	7.8 ± 1.8	4.6 ± 0.5
H34-20K	7.8 ± 0.5	19.7 ± 1.0	145.4 ± 1.5	19.8 ± 1.4	0.06 ± 0.01	18.6 ± 3.5	3.9 ± 0.2
H34-40K	13.7 ± 2.8	23.8 ± 4.0	290.7 ± 132.4	37.7 ± 5.2	0.03 ± 0.01	26.6 ± 4.2	1.5 ± 1.2
H34&E107-5K	5.0 ± 4.8	10.1 ± 2.7	448.1 ± 392.5	9.0 ± 4.2	0.12 ± 0.06	6.3 ± 2.9	4.4 ± 4.4
H34&E107-20K	26.1 ± 3.7	25.3 ± 0.4	425.4 ± 131.9	38.0 ± 7.7	0.03 ± 0.01	26.4 ± 5.3	1.0 ± 0.3

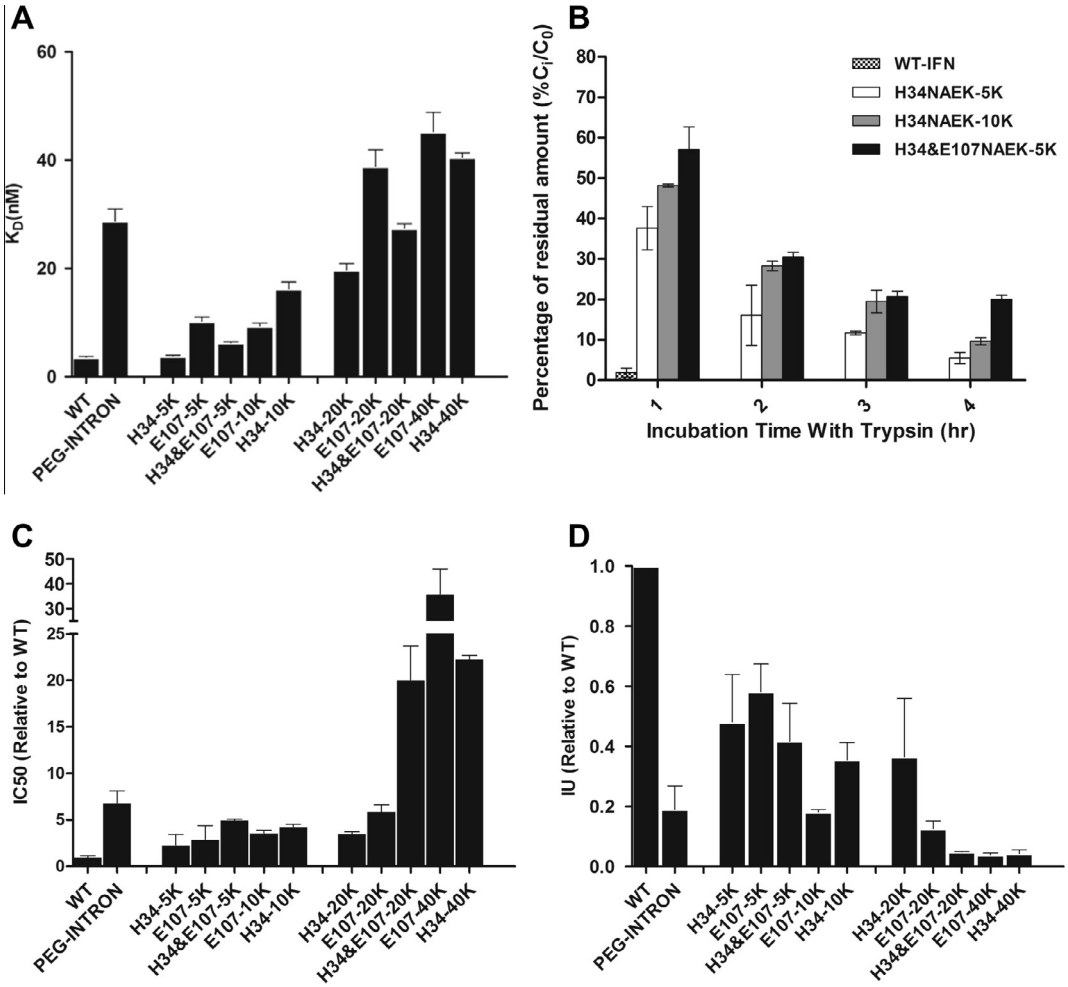

Fig. 5. Comparison of the profiles of mono- vs. dual-PEGylated IFN-α2b s. (A) Affinity (K_D) variation of 5- and 20-kDa dual-PEGylated IFN-α2b s vs. 5-, 10- and 20-kDa mono-PEGylated IFN-α2bs to the receptor. (B) Trypsin digestion resistance of 5-kDa dual-PEGylated IFN-α2b vs. 5- and 10-kDa mono-PEGylated IFN-α2bs. (C) Anti-proliferative and (D) antiviral activity variation of 5- and 20-kDa dual-PEGylated IFN-α2bs vs. 5-, 10-, 20- and 40-kDa mono-PEGylated IFN-α2bs. All quantitative data shown are average values with standard deviations from triplicate experiments ($n = 3$).

4. Discussion

Genetic code expansion refers to an artificial process that uses a stop codon to encode an unnatural amino acid (UAA) at a chosen site of a protein of interest [21,36–39] (Fig. 1). Here, we develop a facile platform through genetic code expansion for site-selective and -specific incorporation of NAEK, a chemical moiety with capability of orthogonal conjugation, into therapeutic IFN-α2b. Our results showed that replacement of a native amino acid with such a Lys-mimicking UAA [23] for most tested sites brings less disruption on both structure and function of IFN-α2b (Fig. 2E). Furthermore, the high fidelity of genetic code expansion allows precise placement of the azido group, and the subsequent orthogonal PEGylation site-specifically and stoichiometrically (Fig. 3A and B). This is superior to the previous methodologies that generally target all active groups of the same type of constitutive amino acids with up to 14 PEGylated positional isomers generated [6,13,14,40], which exhibit activity varying from 1% to 28% comparing with IFN-α2b [5,6,40,41].

The PEGylated IFN-α2b isomers obtained by this approach differ substantially with the commercial PEGylated IFN-α2b in the constituent linker between IFN-α2b and PEG. We take advantage of the incorporated azido group, a critical functional group for a strain-promoted alkyne-azide cycloaddition [24,25], for coupling with an alkyne-containing PEG, which results in the formation of a triazole linker (Fig. 1). The click chemistry-mediated conjugation is temperature- and pH-independent, and is usually accomplished within 1 h (S Fig. 2B). This is superior to the previous methods that utilize the chemistry of succinimidyl carbonate or N-hydroxysuccinimide, which requires stringent conditions, such as a narrow range of pH and temperature and a much longer incubation time, for the formation of a covalent urethane-like or an amide bond linker [7]. In addition, the triazole linker is much more stable under physiological conditions than cysteine-mediated maleimide conjugated linker, which has been utilized successfully for site-specific PEGylation of IFN-α2b.

To identify the favorable site or sites within IFN-α2b and the favorable size of PEG moiety without a significant loss of bioactivities, we re-explored the effects of the PEGylation site and PEG size on IFN-α2b bioactivity. Building on previous works characterizing IFN-α2b-receptor binging interface [17,18,42–46], we chose 20 candidate sites that are mostly located on the protein surface (S Fig. 3), and then evaluated the effect for each NAEK incorporation and subsequent PEG conjugation. Our results indicated most of the chosen sites were functionally tolerant to NAEK replacement and exhibited almost identical activity (Fig. 2E), disclosing the general compatibility of IFN-α2b to NAEK incorporation. R33 is exceptional due to its critical role for binding with IFN-α2b receptor, consistent with the previous report [33]. However, unlike incorporation of NAEK, PEGylation strongly influences the activity of IFN-α2b (Fig. 3C and D). Our approach offered clear advantages for systematic PEGylation of IFN-α2b via NAEK-mediated conjugation of different sizes of PEG at different sites, and thus making it possible to explore the structure–function relationship of PEGylated IFN-α2b. In general, a progressive relationship existed for the decreased bioactivities (Fig. 3D), improved PK properties (Fig. 4A–C and Tables 1–3) and increased PEG sizes, probably due to the less favorable reaction kinetics with the receptor. Changes in the bioactivity appeared to be influenced by the site of PEGylation (Fig. 3C) and the size of the PEG moiety (Fig. 3D). But the circulating half-life varied depending upon the size of the attached PEG moiety rather than the PEGylation site (Fig. 4A–C and Tables 1–3).

Although PEGylation was highly effective for improving PK properties and allowing PEGylated IFN-α2b to achieve long-acting activity, it also attenuated the biological activities with almost a 30-fold loss when modified with a 40-kDa PEG (Fig. 3D), consistent with previous reports [15]. The opposite effects of PEGylation on pharmacokinetics and bioactivity require an optimized balance between improved pharmacokinetic property and reduced bioactivity by the judicious selection of PEG size [47]. As shown in Fig. 3C and D, 10- and 20-kDa PEG- IFN-α2b at H34NAEK and 10-kDa PEG-IFN-α2b at A74NAEK and E107NAEK exhibited the desired biological activity (~30% comparing with IFN-α2b but higher or similar than the marketed PEG-INTRON), the desired clearance half-life (roughly two orders of magnitude of half-life extension comparing with IFN-α2b), and other PK property gains. It seems the most suitable sites for PEGylation are H34NAEK, A74NEAK and E107NAEK; the most proper size of PEG for site H34NAEK is 20-kDa and 10-kDa for A74NEAK and E107NAEK, respectively. It should be noted that H34 is located at a region for interaction with IFNAR2 and thus theoretically not suitable for modification. However, the PEGylated H34NAEK protein was the most active among all positional isomers, and the increase of PEG size from 5 to 20-kDa had little effect on the biological activities (Fig. 3D). This is strikingly different from R33 mutation, a residue also closely located at the same region. For residue R33, a small change like mutation to NAEK depleted the bioactivities of IFN-α2b. It is likely that H34 may not contribute substantially to one of the two putative bindings despite its critical location [11,48].

We also investigated whether the improved property of IFN-α2b by mono-PEGylation could be further improved by dual-PEGylation. To explore such an approach, H34 and E107 were utilized because of their tolerance to mono-PEGylation and their opposite locations. We found di-PEG-IFN-α2b was indeed superior to its mono-PEG derivative in agarose gel shift assay (S Fig. 5A), Biacore affinity test (Fig. 5A), trypsin digestion assay (Fig. 5B) and the anti-proliferation (Fig. 5C) and antivirus assays (Fig. 5D). These results suggest that the effect of a large PEG can be achieved by two smaller PEG moieties. However, significantly diminished bioactivities were observed when two larger sized PEGs as separate moieties were conjugated onto a single IFN-α2b molecule. For example, 15 to 20-fold reduction for 20-kDa PEG was observed. We concluded that PEGylation of IFN-α2b with two or more large PEG molecules, despite the enhanced pharmacological gain, is not favorable for IFN-α2b. It confirmed the superiority of mono-PEGylation and thus the importance of site-selective and -specific PEGylation for the development of next generation IFN-α2b. One remaining question is whether NAEK, upon incorporation into IFN-a2b, has the potential to increase the production of anti-drug antibodies in vivo. Our preliminary studies indicated that parallel injection of NAEK-containing IFN-a2b at either H34 or A74 and wild-type IFN-a2b into rats generated almost the same level of IgG, suggesting that introduction of NEAK into IFN-a2b does not induce immunogenicity. This is not surprising since that the structure of NAEK mimics that of the native amino acid Lys.

5. Conclusion

We report a practical application of genetic code expansion for site-specific PEGylation of IFN-α2b at any chosen site(s), which provides a facile platform for systematic exploration of structure and function of PEGylated IFN-α2b. By this approach, the non-selective conjugation was prevented and a single and homogenous PEGylated IFN-α2b was consistently prepared. Moreover, optimization of the balanced effect of PEGylation on the biological and pharmacological properties of IFN-α2b can be achieved. Upon re-examination of the PEGylated IFN-α2b isomers carrying different sizes of PEG at different sites, we find di- and multi-PEGylation is not a choice for IFN-α2b. More importantly, mono-PEGylates at

H34, A74 and E107 with a 20-, 10- and 10-kDa PEG moiety, respectively, have both higher biological activities and better PK profiles than others. These might represent the direction for development of the next generation of therapeutic IFN-α2b. It is expected that this approach should be suitable for other IFNs and potential protein drugs, as recently reported for human growth hormone [49] and antibody-conjugate drugs [50].

Disclosure of potential conflicts of interest

No potential conflicts of interest were disclosed.

Acknowledgments

We thank Ms. Dan Liu for technical support on mass spectrometric analyses, and Prof. P. Chen for kindly providing plasmids. This work was supported by the National Basic Research Program of China (973 Program; Grant No. 2010CB12300), the National Natural Science Foundation of China (Grants Nos. 81101239, 20932001, 31200568, 91029711, and 20852001), the Research Fund for the Doctoral Program of Higher Education of China (RFDP; Grant Nos. 20110001110054 and 20110001120037) and the Beijing Natural Science Foundation (Grant No. 7153170).

Appendix A. Figures with essential color discrimination

Certain figures in this article, particularly Figs. 1–4 are difficult to interpret in black and white. The full color images can be found in the on-line version, at http://dx.doi.org/10.1016/j.actbio.2015.03.002.

Appendix B. Supplementary data

Supplementary data associated with this article can be found, in the online version, at http://dx.doi.org/10.1016/j.actbio.2015.03.002.

References

[1] Gutterman JU. Cytokine therapeutics: lessons from interferon alpha. Proc Natl Acad Sci USA 1994;91:1198–205.
[2] Pestka S, Krause CD, Walter MR. Interferons, interferon-like cytokines, and their receptors. Immunol Rev 2004;202:8–32.
[3] Borden EC, Sen GC, Uze G, Silverman RH, Ransohoff RM, Foster GR, et al. Interferons at age 50: past, current and future impact on biomedicine. Nat Rev Drug Discovery 2007;6:975–90.
[4] Glue P, Fang JW, Rouzier-Panis R, Raffanel C, Sabo R, Gupta SK, et al. Pegylated interferon-alpha2b: pharmacokinetics, pharmacodynamics, safety, and preliminary efficacy data. Hepatitis C Intervention Therapy Group. Clin Pharmacol Ther 2000;68:556–67.
[5] Grace M, Youngster S, Gitlin G, Sydor W, Xie L, Westreich L, et al. Structural and biologic characterization of pegylated recombinant IFN-alpha2b. J Interferon Cytokine Res 2001;21:1103–15.
[6] Bailon P, Palleroni A, Schaffer CA, Spence CL, Fung WJ, Porter JE, et al. Rational design of a potent, long-lasting form of interferon: a 40 kDa branched polyethylene glycol-conjugated interferon alpha-2a for the treatment of hepatitis C. Bioconjug Chem 2001;12:195–202.
[7] Pfister D, Morbidelli M. Process for protein PEGylation. J Control Release 2014.
[8] Vb D, Cj F. Protein PEGylation: an overview of chemistry and process considerations. Eur Pharm Rev 2010;15(1):18–26.
[9] Veronese FM. Peptide and protein PEGylation: a review of problems and solutions. Biomaterials 2001;22:405–17.
[10] Nairn NW, Shanebeck KD, Wang A, Graddis TJ, VanBrunt MP, Thornton KC, et al. Development of copper-catalyzed azide-alkyne cycloaddition for increased in vivo efficacy of interferon beta-1b by site-specific PEGylation. Bioconjug Chem 2012;23:2087–97.
[11] Grace MJ, Lee S, Bradshaw S, Chapman J, Spond J, Cox S, et al. Site of pegylation and polyethylene glycol molecule size attenuate interferon-alpha antiviral and antiproliferative activities through the JAK/STAT signaling pathway. J Biol Chem 2005;280:6327–36.
[12] Wang YS, Youngster S, Bausch J, Zhang R, McNemar C, Wyss DF. Identification of the major positional isomer of pegylated interferon alpha-2b. Biochemistry 2000;39:10634–40.
[13] Dhalluin C, Ross A, Leuthold LA, Foser S, Gsell B, Muller F, et al. Structural and biophysical characterization of the 40 kDa PEG-interferon-alpha2a and its individual positional isomers. Bioconjug Chem 2005;16:504–17.
[14] Wang YS, Youngster S, Grace M, Bausch J, Bordens R, Wyss DF. Structural and biological characterization of pegylated recombinant interferon alpha-2b and its therapeutic implications. Adv Drug Deliv Rev 2002;54:547–70.
[15] Monkarsh SP, Ma Y, Aglione A, Bailon P, Ciolek D, DeBarbieri B, et al. Positional isomers of monopegylated interferon alpha-2a: isolation, characterization, and biological activity. Anal Biochem 1997;247:434–40.
[16] Pasut G, Veronese FM. State of the art in PEGylation: the great versatility achieved after forty years of research. J Control Release 2012;161:461–72.
[17] Rosendahl MS, Doherty DH, Smith DJ, Carlson SJ, Chlipala EA, Cox GN. A long-acting, highly potent interferon alpha-2 conjugate created using site-specific PEGylation. Bioconjug Chem 2005;16:200–7.
[18] Bell SJ, Fam CM, Chlipala EA, Carlson SJ, Lee JI, Rosendahl MS, et al. Enhanced circulating half-life and antitumor activity of a site-specific pegylated interferon-alpha protein therapeutic. Bioconjug Chem 2008;19:299–305.
[19] Shen BQ, Xu K, Liu L, Raab H, Bhakta S, Kenrick M, et al. Conjugation site modulates the in vivo stability and therapeutic activity of antibody–drug conjugates. Nat Biotechnol 2012;30:184–9.
[20] Jackson D, Atkinson J, Guevara CI, Zhang C, Kery V, Moon SJ, et al. In vitro and in vivo evaluation of cysteine and site specific conjugated herceptin antibody-drug conjugates. PLoS One 2014;9:e83865.
[21] Wang L, Brock A, Herberich B, Schultz PG. Expanding the genetic code of *Escherichia coli*. Science 2001;292:498–500.
[22] Deiters A, Cropp TA, Summerer D, Mukherji M, Schultz PG. Site-specific PEGylation of proteins containing unnatural amino acids. Bioorg Med Chem Lett 2004;14:5743–5.
[23] Nguyen DP, Lusic H, Neumann H, Kapadnis PB, Deiters A, Chin JW. Genetic encoding and labeling of aliphatic azides and alkynes in recombinant proteins via a pyrrolysyl-tRNA synthetase/tRNA(CUA) pair and click chemistry. J Am Chem Soc 2009;131:8720–1.
[24] Chang PV, Prescher JA, Sletten EM, Baskin JM, Miller IA, Agard NJ, et al. Copper-free click chemistry in living animals. Proc Natl Acad Sci USA 2010;107:1821–6.
[25] Mbua NE, Guo J, Wolfert MA, Steet R, Boons GJ. Strain-promoted alkyne-azide cycloadditions (SPAAC) reveal new features of glycoconjugate biosynthesis. Chembiochem 2011;12:1912–21.
[26] Lallana E, Riguera R, Fernandez-Megia E. Reliable and efficient procedures for the conjugation of biomolecules through Huisgen azide-alkyne cycloadditions. Angew Chem 2011;50:8794–804.
[27] Valente CA, Prazeres DM, Cabral JM, Monteiro GA. Translational features of human alpha 2b interferon production in *Escherichia coli*. Appl Environ Microbiol 2004;70:5033–6.
[28] Schmeisser H, Kontsek P, Esposito D, Gillette W, Schreiber G, Zoon KC. Binding characteristics of IFN-alpha subvariants to IFNAR2-EC and influence of the 6-histidine tag. J Interferon Cytokine Res 2006;26:866–76.
[29] Kim YM, Lee HJ, Lee JE, Kim HY, Kim J. Expression of human interferon alpha-1 with enhanced stability via the tagging system of a stabilizing peptide. Protein Expr Purif 2009;63:140–6.
[30] Ramon J, Saez V, Baez R, Aldana R, Hardy E. PEGylated interferon-alpha2b: a branched 40K polyethylene glycol derivative. Pharm Res 2005;22:1374–86.
[31] Rabhi-Essafi I, Sadok A, Khalaf N, Fathallah DM. A strategy for high-level expression of soluble and functional human interferon alpha as a GST-fusion protein in *E. coli*. Protein Eng Des Sel 2007;20:201–9.
[32] Villaverde A, Carrio MM. Protein aggregation in recombinant bacteria: biological role of inclusion bodies. Biotechnol Lett 2003;25:1385–95.
[33] Camble R, Petter NN, Trueman P, Newton CR, Carr FJ, Hockney RC, et al. Functionally important conserved amino-acids in interferon-alpha 2 identified with analogues produced from synthetic genes. Biochem Biophys Res Commun 1986;134:1404–11.
[34] Novick D, Cohen B, Rubinstein M. The human interferon alpha/beta receptor: characterization and molecular cloning. Cell 1994;77:391–400.
[35] Kaminskas LM, Ascher DB, McLeod VM, Herold MJ, Le CP, Sloan EK, et al. PEGylation of interferon alpha2 improves lymphatic exposure after subcutaneous and intravenous administration and improves antitumour efficacy against lymphatic breast cancer metastases. J Control Release 2013;168:200–8.
[36] Chin JW, Cropp TA, Anderson JC, Mukherji M, Zhang Z, Schultz PG. An expanded eukaryotic genetic code. Science 2003;301:964–7.
[37] Song W, Wang Y, Qu J, Lin Q. Selective functionalization of a genetically encoded alkene-containing protein via "photoclick chemistry" in bacterial cells. J Am Chem Soc 2008;130:9654–5.
[38] Wang YS, Fang X, Wallace AL, Wu B, Liu WR. A rationally designed pyrrolysyl-tRNA synthetase mutant with a broad substrate spectrum. J Am Chem Soc 2012;134:2950–3.
[39] Hino N, Okazaki Y, Kobayashi T, Hayashi A, Sakamoto K, Yokoyama S. Protein photo-cross-linking in mammalian cells by site-specific incorporation of a photoreactive amino acid. Nat Methods 2005;2:201–6.
[40] Foser S, Schacher A, Weyer KA, Brugger D, Dietel E, Marti S, et al. Isolation, structural characterization, and antiviral activity of positional isomers of monopegylated interferon alpha-2a (PEGASYS). Protein Expr Purif 2003;30:78–87.
[41] Zeuzem S, Feinman SV, Rasenack J, Heathcote EJ, Lai MY, Gane E, et al. Peginterferon alfa-2a in patients with chronic hepatitis C. N Engl J Med 2000;343:1666–72.

[42] Akabayov SR, Biron Z, Lamken P, Piehler J, Anglister J. NMR mapping of the IFNAR1-EC binding site on IFNalpha2 reveals allosteric changes in the IFNAR2-EC binding site. Biochemistry 2010;49:687–95.
[43] Nudelman I, Akabayov SR, Schnur E, Biron Z, Levy R, Xu Y, et al. Intermolecular interactions in a 44 kDa interferon-receptor complex detected by asymmetric reverse-protonation and two-dimensional NOESY. Biochemistry 2010;49:5117–33.
[44] Thomas C, Moraga I, Levin D, Krutzik PO, Podoplelova Y, Trejo A, et al. Structural linkage between ligand discrimination and receptor activation by type I interferons. Cell 2011;146:621–32.
[45] Radhakrishnan R, Walter LJ, Hruza A, Reichert P, Trotta PP, Nagabhushan TL, et al. Zinc mediated dimer of human interferon-alpha 2b revealed by X-ray crystallography. Structure 1996;4:1453–63.
[46] Hopp TP, Woods KR. Prediction of protein antigenic determinants from amino acid sequences. Proc Natl Acad Sci USA 1981;78:3824–8.
[47] Jo YW, Youn YS, Lee SH, Kim BM, Kang SH, Yoo M, et al. Long-acting interferon-alpha 2a modified with a trimer-structured polyethylene glycol: preparation, in vitro bioactivity, in vivo stability and pharmacokinetics. Int J Pharm 2006;309:87–93.
[48] Grace MJ, Cutler D. Pegylating IFNs at his-34 improves the in vitro antiviral activity through the JAK/STAT pathway. Antiviral Chem Chemother 2004;15:287–97.
[49] Cho H, Daniel T, Buechler YJ, Litzinger DC, Maio Z, Putnam AM, et al. Optimized clinical performance of growth hormone with an expanded genetic code. Proc Natl Acad Sci USA 2011;108:9060–5.
[50] Tian F, Lu Y, Manibusan A, Sellers A, Tran H, Sun Y, et al. A general approach to site-specific antibody drug conjugates. Proc Natl Acad Sci USA 2014;111:1766–71.